Atomic-level study on the interaction of plastic slip with Σ3{112} tilt grain boundary and {112} twins in bcc metals

N. Kvashin,[1,*] N. Anento,[1] D. Terentyev,[2] and A. Serra[1]
[1]*Department of Civil and Environmental Engineering, Universitat Politècnica de Catalunya, 08034 Barcelona, Spain*
[2]*SCK.CEN, Nuclear Materials Science Institute, Boeretang 200, B-2400 Mol, Belgium*

(Received 20 July 2021; accepted 7 March 2022; published 25 March 2022)

The Σ3{112} tilt grain boundary (GB) is found in many grains in bcc polycrystalline metals due to its low energy and high stability. Moreover, it is the coherent boundary of the {112} twin. This paper studies the interaction of a pileup of 1/2⟨111⟩ dislocations with the {112} GB, extendable to the coherent {112} twin boundary (TB). The results are applied to the interaction of the pileup of dislocations with the {112} twin. The interacting dislocation is transformed into a GB dislocation (or TB dislocation) that acts as a source of disconnections responsible for the shear-coupled GB migration leading to twin growth or shrinkage when the interface is a TB. While a single dislocation cannot be transmitted through the interface, the stress field of the pileup facilitates the transmission if the tensile part of the dislocation core is closer to the interface than the compression part. The {112} twin is found to create barriers to the motion of 1/2⟨111⟩ crystal dislocations, and the strength of the barrier depends on crystallographic parameters. The results obtained in the slip-TB interaction prove that there is no transmission of dislocations through the twin. Thus, under twinning shear stress, all twins are strong obstacles for the glide of dislocations. Under antitwinnning shear stress, twins with thickness less than a few nanometers (5.6 nm in Fe) are annihilated by the interaction with a pileup of dislocations, contributing to softening, whereas thicker twins block the propagation of dislocations and confine dislocations inside the twin, which contributes to hardening.

DOI: 10.1103/PhysRevMaterials.6.033606

I. INTRODUCTION

The accommodation of plastic deformation in polycrystalline materials, such as metals and metallic alloys, occurs through the motion of dislocations, the creation and growth of twins, and the displacement of interfaces, such as grain boundaries (GBs) and twin boundaries (TBs) [1–3]. The dynamics of these defects implies their mutual interactions, which, in turn, determine the macroscopic properties of polycrystals under applied thermal and/or mechanical treatment. While the initiation of plastic deformation is controlled by the motion of dislocations, the sustainability and capacity of microscopically homogeneous deformation is defined by the propagation of slip through grains [1,4], their interactions inside the grain with other defects [5], and the slip-twin interactions [6–12].

Structural materials for high-demand or extreme applications (e.g., space, high pressure, fast deformation, a harsh nuclear environment) are required to exhibit high strength and ductility at the same time, which is challenging. Because of their high strength and acceptable cost, bcc metals are often used as a basis. Under quasistatic and moderate-speed dynamic loads, plastic deformation is controlled by the activation of screw dislocations, interaction between dislocations, and interaction of dislocation pileups with grain boundaries and eventually grain boundary slip, as the ambient temperature is sufficiently high. However, under high speed or shock-compressed deformation (as in the case of accidents or transient regimes) the formation of twins coexists with the regular dislocation multiplication [13]. Understanding the mechanisms of fast deformation has important consequences for practical applications such as the development of impact-resistant armor and also has fundamental relevance, e.g., in investigations of the state of matter during planetary collisions in space [14,15].

It is known that the interaction of a slip system with a GB is specific to each GB. It depends mainly on two factors: (i) the atomic configuration of the GB and the orientation of the Burgers vector of the dislocations and (ii) the local stress in the interaction region.

(i) The dislocation at the GB undergoes a variety of feasible processes. The possible reactions of the dislocation present a gradation of complexity, ranging from transmission with a small resistance keeping the same Burgers vector [16] to full absorption by the GB [17,18]. In intermediate situations, the dislocation is partially transmitted, leaving a residual defect at the GB, which is necessary to account for Burgers vector conservation [19]. An extreme case is presented by GBs that are impenetrable obstacles for the glide of dislocations; then, the dislocation is neither transmitted nor absorbed [20]. In partial (total) absorption of the dislocation by the interface, the dislocation is partially (totally) transformed into either GB dislocations (GBDs) at the GB or TB dislocations (TBDs) at the TB. The GBDs and TBDs that step the interface are named disconnections (interfacial line defects with both dislocation and step character [21,22]); among them, we distinguish the gliding elementary disconnections (EDisc) [23], with the

*nikolai.kvashin@upc.edu

Burgers vector parallel to the interface, which are responsible for the shear-coupled boundary migration [17,18,23–29] and for the twin growth [30]. The GBDs could favor either the shear-coupled GB migration or the nucleation of other defects such as twins [31–33] and dislocations [34]; this behavior occurs in GBs of the most common crystallographic structures in metals, i.e., bcc, fcc, and hcp [23–37].

(ii) The influence of the local shear stress is evidenced by comparing the interaction of a single dislocation with the interaction of a pileup of dislocations since for the latter the local shear stress at the interaction region is dominated by the incoming dislocations. An illustrative example of the above-described behavior is the interaction of dislocations with a symmetric $\{332\}\langle 110\rangle$ tilt GB studied by molecular dynamics simulation [31,32]. In fact, the $\{332\}$ GB absorbs $1/2\langle 111\rangle$ crystal dislocations, transforming them into disconnections which modify the GB shape, but there is no transmission of the dislocations to the adjacent grain. In such GBs, the behavior of GBDs under shear stress depends on the orientation of the Burgers vector and sense of shear stress. In the interaction of the $\Sigma 11\{332\}$ GB with a single dislocation [31], there are two cases: (i) The GBD moves conservatively (no atomic diffusion is needed) together with the GB, acting as a source of disconnections; consequently, plastic deformation is accommodated by shear-coupled GB migration. (ii) The GBD is sessile; if so, the GBD becomes the nucleus of a $\{112\}$ twin. Then, in the presence of $\{332\}$ GBs, plastic deformation is accommodated by the combination of the motion of the $\{332\}$ GB and the growth of $\{112\}$ twins inside the grain. If a pileup of dislocations interacts with the GB [32], a disconnection with a much larger stepped core is formed by absorption of the dislocations of the pileup, which forms a new asymmetric GB $\{112\}/\{110\}$. In this case no twins are formed. Thus, the stress field of the dislocation pileup may affect the result of the interaction.

In experiments on the dislocation – individual grain boundary interactions have evidenced the specificity of each interaction. Recently, Weaver *et al.* [38] reported the first bcc bicrystal pillar compression test conducted on a tantalum bicrystal to investigate the slip transmission across three high-angle GBs. They evidenced different behavior of each boundary to the stress-strain response and slip transmissibility.

At the atomic scale, within the delimited volumes of the dislocation interaction, when the width of the twin is large enough to avoid the influence of the other coherent TB, the interaction of a dislocation with the coherent interface of a twin is equivalent to the interaction with the corresponding tilt GB. TBs can effectively strengthen materials by impeding dislocation motion and increasing the ductility and work-hardening capability of twinned metallic materials [12]. The slip-twin interaction and its dependence on the width of the twin have been largely studied for fcc nanotwinned metals [7–11]. Experiments on nanotwinned copper [11] demonstrated that the strength of nanotwinned metals with equiaxed grains reaches a maximum value at a critical twin size of a few nanometers, below which the strength decreases with the TB spacing. Whereas the dislocation-TB interaction is well described for fcc metals, there are scarce studies concerning twinning in bcc metals, characterized by the simultaneous concurrence of two deformation modes, namely, the $\{112\}$ twinning and $1/2\langle 111\rangle$ slip, leading to twin-slip interaction [39–45]. A detailed description at the atomic level of the mechanisms of the interaction would contribute to the understanding of the strain hardening and ductility of bcc metals.

The study presented in [18] reported that a single crystal dislocation under stress might be absorbed by the $\{112\}$ interface but there is no transmission through the interface. This behavior changes if other dislocations, gliding along the same glide plane, approach the $\{112\}$ GB. The present paper explores the reaction at the $\{112\}$ interface if the interaction is produced by a dislocation pileup (DPU) and applies the results to a subsequent analysis of the twin-slip interaction.

This paper is structured as follows: Sec. II provides a description of the simulation method. Section III synthesizes the main features of the interaction of a single dislocation with the $\{112\}$ GB, while Sec. IV presents the results on both the interaction of the $\{112\}$ GB with a DPU and the slip-twin interaction. Finally, in Secs. V and VI we present the discussion and the main conclusions.

This study mainly focuses on bcc Fe, although to understand the effect of the interatomic forces on the different processes studied, we compare the main features found in Fe with the interaction in Cr and W, two bcc metals with wide application in the energy sector, in particular as structural materials for nuclear and space applications.

II. METHODOLOGY

The present atomistic calculations were performed using supercells containing two grains of bcc metal. The principal axes x, y, and z of the upper crystal λ were oriented along the $[1\bar{1}1]$, $[110]$, and $[1\bar{1}2]$ directions, respectively, while for the lower crystal μ the axes were mirror reflected. Each simulation started with a static relaxation, i.e., energy minimization, which was performed while applying periodic boundary conditions along the x and y directions and fixed boundaries perpendicular to the GB plane.

The molecular dynamics (MD) simulation box consisted of a symmetric bicrystal with an initially coherent GB interface in the middle. Approximate dimensions of the cell size were $160 \times 4 \times 80$ lattice vectors along the corresponding directions with a total number of atoms $N \sim 600\,000$. The crystal dislocations of the pileup are introduced along $\{112\}$ glide planes for edge dislocations and along a $\{110\}$ plane for the mixed dislocation. For a given glide plane inclination, we consider, in turn, two dislocations with opposite senses of their Burgers vectors, i.e., pointing away from the interface and pointing toward it. The MD simulation is performed using LAMMPS with periodic boundary conditions along the tilt axis and fixed conditions in the other two directions.

The interatomic interactions in iron were modeled by using the embedded-atom method potential by Ackland *et al.* [46], fitted to reproduce properties of dislocation lines obtained from density functional theory (DFT). The accuracy of the potential in the study of $\langle 110\rangle$ tilt GBs was checked in [47]. For chromium, the potential derived by Bonny *et al.*, fitted to thermodynamic and point-defect properties obtained from

DFT calculations and experiments, was used [48]. As for tungsten, the potential developed by Marinica *et al.* was chosen [49]. This potential is fitted to a mixed database containing various experimentally measured properties of tungsten and *ab initio* formation energies of defects. The stress state of the system was recorded after each increment of strain. The open visualization tool OVITO was used for visualization and analysis of atomistic simulation data [50].

GB-DPU interactions were modeled by using a hybrid model combining atomistic and continuous approaches, initially described in [51] and applied in [32,52]. In the continuum region, the positions of the dislocations are calculated as a function of the external stress σ, number of dislocations in the pileup n, and the position of the heading dislocation that is held fixed, according to the expression $n = L\sigma/A$ [53], where L is the total distance between the first and last dislocations and A is a parameter depending on the Burgers vector, the character of the dislocation, and the material. The displacement field is then applied to the previously defined atomistic simulation cell, formed by two regions, namely, an inner region of mobile atoms and an outer region of fixed atoms. The continuum approach is used to define the atomistic displacements, at each increment of stress, applied in the outer region, emulating the increase of stress. The inner region of atoms is evolved by molecular dynamics at different temperatures.

The bicrystals were relaxed using the conjugate gradient method, and then atomic displacements were applied to all the atoms of the simulation cell, corresponding to an initial applied stress. The crystal was relaxed again and thermalized for 20 ps to achieve a desired initial temperature. A fixed integration MD time step of 1 fs was used for all runs.

The shear stress was applied along the glide plane of the DPU, thereby favoring the motion of DPU toward the interface. To mimic the increase of shear stress, the atomic positions of the outer region were updated. With respect to the loading conditions, the following parameters were fixed: the number of dislocations in the pileup (15 units), the increment of the externally applied stress ($\Delta\sigma_{\text{app}} = 100$ MPa), and the maximum of the externally applied stress ($\sigma_{\text{app,max}} = 5.5$ GPa).

The simulation temperature ranged from 300 to 900 K, thus enhancing or reducing the role played by thermal activation. Since the local atomic configuration at the GB is different for the two adjacent glide planes (see dashed lines A and B in Fig. 1), the study was extended to both glide planes.

For the sake of favoring the creation and propagation of EDisc, a test was performed in Fe at $T = 300$ K by applying a shear stress parallel to the GB. The initial thermalized configuration obtained with the hybrid method was deformed quasistatically. Each increment of strain was introduced by applying deformation to the whole box parallel to the GB plane followed by energy minimization. The same configuration and shear strain were applied to study the interaction of the $\mathbf{b}_{\pm 2/0}$ pileup with a $(1\bar{1}2)$ twin.

Finally, in order to check the effect of the LAMMPS box thickness on the relaxation mechanisms we performed several simulations with the thickness increased to 60 lattice parameters along the [110] directions. The effect on the reaction mechanisms and stresses was found to be negligible.

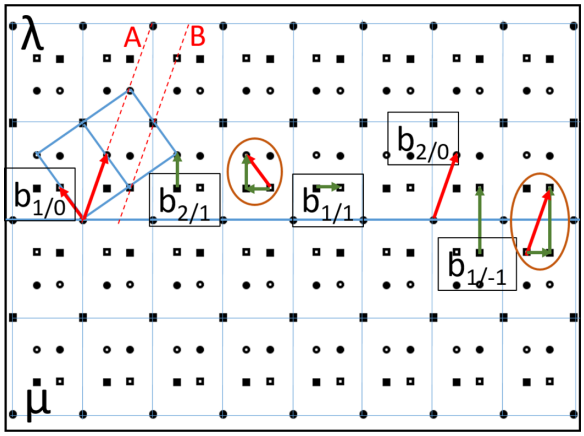

FIG. 1. Projection along the [110] tilt axis of the dichromatic pattern associated with the $(1\bar{1}2)$ GB showing the Burgers vectors of interfacial defects (green arrows), crystal dislocations of the λ crystal (red arrows), and two adjacent glide planes of edge dislocations (red dashed lines).

III. SUMMARY OF THE INTERACTION OF A SINGLE DISLOCATION WITH THE {112} TILT GB

A. Dichromatic pattern

To describe the relationship between the crystal dislocations and the GBDs we use the dichromatic pattern shown in Fig. 1.

The dichromatic pattern is formed by the projection, along the [110] tilt axis, of the lattice sites of the two crystals, namely, λ (white) and μ (black), with the $(1\bar{1}2)$ plane in coincidence. The Burgers vectors of interfacial dislocations are represented by vectors from black to white sites. The notation $\mathbf{b}_{n/m}$ used to describe the Burgers vectors indicates that the core of the corresponding boundary line defect steps the GB by n $(1\bar{1}2)$ planes of the λ crystal and m $(1\bar{1}2)$ planes of the μ crystal. On any reaction, in addition to Burgers vector conservation, there is also conservation of the indices n and m. This notation is extended to crystal dislocations as $\mathbf{b}_{n/0}$ and $\mathbf{b}_{0/m}$ in the λ and μ crystals, respectively. The EDisc, identified as $\mathbf{b}_{\pm 1/\pm 1}$, have a Burgers vector parallel to the GB with a magnitude 1/3 of the crystal dislocation Burgers vector, i.e., $\mathbf{b} = \frac{1}{6}[1\bar{1}\bar{1}]$.

B. Elementary disconnections at the (112) GB

Besides the low formation energy of the {112} tilt GB, a relevant feature of this GB for the accommodation of plastic deformation is the existence of highly glissile EDiscs responsible for the shear-coupled GB migration [17,18,24,25]. The critical resolved shear stress of the EDisc is about 20 MPa [54] in Fe. These EDisc are created either as dipole pairs in the pristine interface under shear stress, as shown in Fig. 2, or by sources of disconnections such as the GBD created during the interaction with a crystal dislocation [18], as detailed below.

C. Single dislocation interaction with the {112} grain boundary

The edge dislocation $\mathbf{b}_{-2/0} = \frac{1}{2}[\bar{1}1\bar{1}]$ is attracted by the $(1\bar{1}2)$ GB, and the outcome of the interaction is the absorption

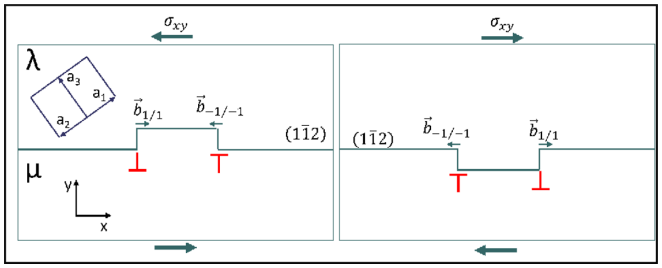

FIG. 2. Schematic of the bicrystal containing a {112} GB showing the unit cell of the upper crystal λ and the EDisc dipoles created under applied shear stress.

of the dislocation by the GB along with the creation of a GBD $\mathbf{b}_{-1/1} = \frac{1}{3}[\bar{1}1\bar{2}]$ that does not step the boundary and the emission of an EDisc that glides away. The reaction describing this process is $\mathbf{b}_{-2/0} = \mathbf{b}_{-1/1} + \mathbf{b}_{-1/-1}$

The GBD $\mathbf{b}_{-1/1}$ acts as a source of pairs of disconnections of opposite sign that are created on each side of the GBD. The glide of these EDisc displaces the GB one plane, producing shear-coupled GB migration. The GBD moves together with the GB by a conservative climb (see [18] for details), such that the creation of EDisc's is sustained. Moreover, the interaction with other EDisc's, approaching the GBD, is conservative; therefore, all EDisc's gliding along the GB contribute efficiently to the displacement of the GB [18].

The dislocation $\mathbf{b}_{2/0} = \frac{1}{2}[1\bar{1}1]$ is repelled by the $(1\bar{1}2)$ GB. Under an applied stress, the repulsion of the $\mathbf{b}_{2/0}$ dislocation triggers the creation of dipoles of EDisc on the interface whose glide produces the migration of the GB while the $\mathbf{b}_{2/0}$ dislocation keeps gliding in the λ crystal following the GB.

The mixed dislocation $\mathbf{b}_{\pm1/0}$ also keeps its own Burgers vector, and it is dragged by the GB during the shear-coupled GB migration. In summary, no transmission of a single dislocation through the {112} GB is produced.

IV. RESULTS

The first part of this section describes the interaction of a DPU of $1/2\langle111\rangle$ dislocations with the $(1\bar{1}2)\langle110\rangle$ tilt interface. At the atomic scale, within the delimited volumes of the dislocation interaction, the interface can be understood as a grain boundary as well as a twin boundary. Thus, Sec. IV A describes the slip transfer conditions at the {112} GB, and Sec. IV B describes the slip-twin interaction, i.e., the interaction of the DPU with a $(1\bar{1}2)$ twin, which is directly related to the results of the first part.

A. DPU-GB interaction

The pileup of crystal dislocations considered for the interaction with the $(1\bar{1}2)$ GB are the edge $\mathbf{b}_{\pm2/0} = \pm\frac{1}{2}[1\bar{1}1]$ gliding along the $(\bar{1}12)$ plane inclined at 70.53° with the GB and the mixed $\mathbf{b}_{\pm1/0} = \pm\frac{1}{2}[111]$ gliding along the $(1\bar{1}0)$ plane inclined at 125.26° with the GB. They are represented (red arrows) in the dichromatic pattern in Fig. 1 together with the interfacial defects: EDisc $\mathbf{b}_{1/1} = \frac{1}{6}[1\bar{1}\bar{1}]$, the disconnection $\mathbf{b}_{2/1} = \frac{1}{3}[121]$, and the GBD $\mathbf{b}_{1/-1} = \frac{1}{3}[1\bar{1}2]$ that does not step the GB (green arrows). Except in Sec. IV A 4, the external shear stress was applied along the glide plane of the DPU.

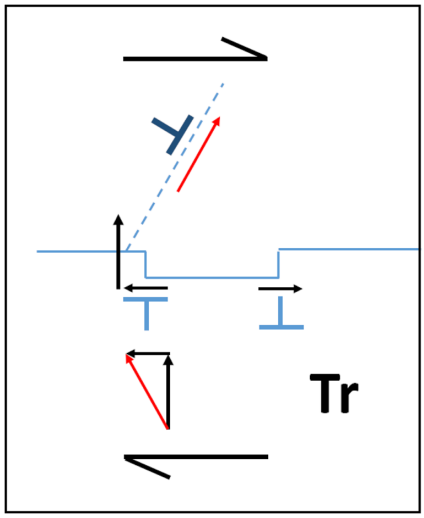

FIG. 3. Schematic showing the production of an EDisc dipole under external stress (big black arrows at the top and the bottom show the component parallel to the GB) leading to a transmission reaction (Tr). Red arrows indicate the Burgers vectors of the incident and transmitted crystal dislocations, and black arrows show the Burgers vector of the EDisc and the GBD.

1. *Interaction of the* $(1\bar{1}2)$ *GB with the pileup of edge dislocations* $\mathbf{b}_{2/0}$

The Burgers vector (upper red arrow in Fig. 3) of the $\mathbf{b}_{2/0}$ dislocations is pointing away from the interface. When the DPU is few lattice parameters away from the GB, the heading dislocation is attracted and absorbed by the GB according to the following reaction: $\frac{1}{2}[1\bar{1}1]_\lambda = \frac{1}{3}[1\bar{1}2]_\lambda + \frac{1}{6}[1\bar{1}\bar{1}]_\lambda$, written in coordinates of the upper crystal λ. The absorption, not observed for the single dislocation, is mediated by the stress field produced by the trailing dislocations of the DPU.

Under an applied shear stress, a dipole of disconnections is created at the GB on the right side of the GBD (see Fig. 3), which is the tensile region of the trailing dislocations. Then, the EDisc that approaches the GBD is $\mathbf{b}_{-1/-1} = \frac{1}{6}[\bar{1}11]$, and the reaction is

$$\tfrac{1}{3}[1\bar{1}2]_\lambda + \tfrac{1}{6}[\bar{1}11]_\lambda = \tfrac{1}{6}[1\bar{1}5]_\lambda = \tfrac{1}{2}[\bar{1}11]_\mu = \mathbf{b}_{0/2}. \quad (1)$$

Therefore, the dislocation has changed the orientation of the Burgers vector, making it able to glide into the lower crystal μ; that is, the dislocation has been *transmitted*. As the transmitted dislocation moves downward, the other EDisc of the dipole has glided away along the GB, leaving a pristine interface for the second dislocation of the pileup, which, in turn, is absorbed, as was the first dislocation.

Although the atomic distributions at the intersection of neighboring glide planes with the GB are not identical (see red dashed lines A and B in Fig. 1), the transmission of dislocations occurs in both glide planes.

The transmission occurs when the stress field of the DPU can supply the threshold shear stress in the vicinity of the GBD for the dipole to be created, as detailed in Table I.

TABLE I. Local shear stress at the reaction site necessary for triggering a reaction at the interface for the edge dislocations in Fe.

$\mathbf{b}_{2/0}$			
Temperature (K)	Compression region (MPa)	Tension region (MPa)	Scheme
300	795	−1385	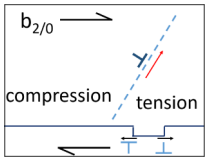
450	794	−1371	
600	789	−1353	
750	771	−1324	
900	730	−1323	
$\mathbf{b}_{-2/0}$			
Temperature (K)	Tension region (MPa)	Compression region (MPa)	Scheme
300	1524	−594	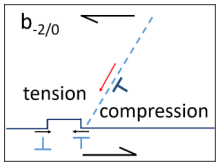
600	1202	−590	
900	1070	−543	

2. *Interaction of the* $(1\bar{1}2)$ *GB with the pileup of edge dislocations* $\mathbf{b}_{-2/0}$

The Burgers vector of the $\mathbf{b}_{-2/0}$ dislocations is pointing toward the interface (upper red arrow in Fig. 4). The heading dislocation of the pileup is absorbed by the GB according to the following reaction: $\frac{1}{2}[\bar{1}1\bar{1}]_\lambda = \frac{1}{3}[\bar{1}1\bar{2}]_\lambda + \frac{1}{6}[\bar{1}11]_\lambda$, written in coordinates of the upper crystal λ. The EDisc ($\frac{1}{6}[\bar{1}11]_\lambda$) glides away, and the GBD ($\frac{1}{3}[\bar{1}1\bar{2}]_\lambda$) does not step the GB.

Under the stress field of the trailing dislocations, a dipole of EDisc is created at the GB on the left side of the GBD, which is the tensile region of the trailing dislocations, as shown in Fig. 4. Then, the disconnection that approaches the GBD is $\frac{1}{6}[\bar{1}11]_\lambda$, and the reaction is $\frac{1}{3}[\bar{1}1\bar{2}]_\lambda + \frac{1}{6}[\bar{1}11]_\lambda = \frac{1}{2}[\bar{1}1\bar{1}]_\lambda = \mathbf{b}_{2/0}$. The orientation of the Burgers vector is not favorable to the glide on the lower crystal, and the result is the migration of the GB into the λ crystal against the DPU.

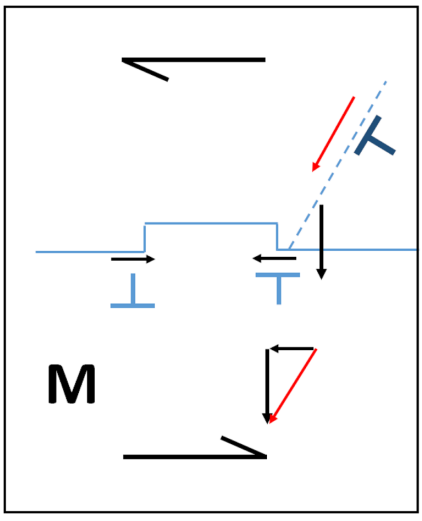

FIG. 4. Schematic showing the production of an EDisc dipole under external stress (big black arrows at the top and the bottom show the component parallel to the GB) leading to a migration (M) of the GB. Red arrows indicate the Burgers vectors of the incident crystal dislocations, and black arrows show the Burgers vector of the EDisc and the GBD.

Figures 3 and 4 show that the reaction is controlled by the location of the created EDisc dipoles, which determines whether the dislocation can be transmitted. Since the creation of dipoles is stress dependent, the shear stress on both sites of the interaction region, corresponding to the tension and compression regions of the dislocation core, were calculated. Table I shows the local shear stress parallel to the GB in each side of the interaction region for $\mathbf{b}_{2/0}$ and $\mathbf{b}_{-2/0}$, as shown by the schemes. Only the tension region experiences enough shear stress for the dipole to be created, and the sense of the shear determines whether the dipole displaces the GB upward or downward. The local shear stresses for $\mathbf{b}_{2/0}$ diminish slightly with increasing the temperature. The decreasing of stress is more pronounced for $\mathbf{b}_{-2/0}$.

3. *Interaction of the* $(1\bar{1}2)$ *GB with the pileup of mixed dislocations* $\mathbf{b}_{\pm 1/0}$

The mixed dislocations glide on the $(1\bar{1}0)$ plane that forms an angle of 125.26° with the GB. The Burgers vectors of the dislocations of the pileup are $\mathbf{b}_{-1/0} = \frac{1}{2}[\bar{1}\bar{1}\bar{1}]_\lambda$ and $\mathbf{b}_{1/0} = \frac{1}{2}[111]_\lambda$.

For the mixed dislocation, there is only absorption of the first dislocation of the DPU. No other reactions were observed at any temperature up to the maximum stress applied. The reactions of $\mathbf{b}_{1/0}$ and $\mathbf{b}_{-1/0}$ are described, respectively, in the following equations and plotted schematically in Fig. 1:

$$\begin{aligned} \tfrac{1}{2}[111]_\lambda &= \tfrac{1}{3}[121]_\lambda + \tfrac{1}{6}[1\bar{1}1]_\lambda, \\ \tfrac{1}{2}[\bar{1}\bar{1}\bar{1}]_\lambda &= \tfrac{1}{3}[\bar{1}\bar{2}\bar{1}]_\lambda + \tfrac{1}{6}[\bar{1}1\bar{1}]_\lambda, \end{aligned} \tag{2}$$

where $\frac{1}{3}[121]_\lambda = \mathbf{b}_{2/1}$ and $\frac{1}{3}[\bar{1}\bar{2}\bar{1}]_\lambda = \mathbf{b}_{-2/-1}$ are disconnections (GBDs that step the GB) that can be described as a sum of edge and screw parts: $\frac{1}{6}[\bar{1}12]_\lambda + \frac{1}{2}[110]_\lambda$ and $\frac{1}{6}[1\bar{1}\bar{2}]_\lambda + \frac{1}{2}[\bar{1}\bar{1}0]_\lambda$, respectively.

4. *Interaction under a shear stress parallel to the* $(1\bar{1}2)$ *GB at 300 K*

Our results show that the reactions are controlled by the creation and propagation of EDisc; therefore, an applied shear stress parallel to the GB would optimize the production of dipoles of EDisc and subsequently would reduce the applied stress necessary for the reaction at the GB to be produced.

To check this hypothesis, an external shear stress parallel to the GB was applied to a bicrystal at 300 K. The results prove that both transmission and interface displacement are produced at lower stresses.

This implies that the transmission of dislocations is more efficient, and with the stress applied parallel to the GB for the $\mathbf{b}_{2/0}$ DPU, we observe the consecutive transmissions of every dislocation from the DPU (Fig. 5), while for a stress parallel to the glide plane, the level of stresses for the second and further dislocations to be transmitted was not reached within the maximum shear stress applied.

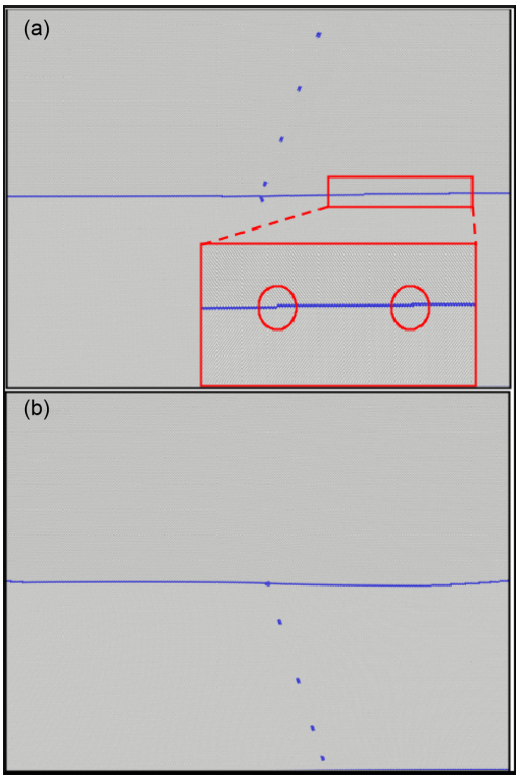

FIG. 5. Interaction of a pileup of edge dislocations with the $(1\bar{1}2)$ GB. (a) Interaction of the first dislocation. Inset: detail of the EDisc emitted during the interaction. (b) Transmitted pileup of dislocations. The remaining EDisc are piling up at the right fixed boundary of the simulated system.

Figure 5 shows the transmission of a pileup of five $\mathbf{b}_{2/0}$ dislocations under a shear parallel to the GB. In Fig. 5(a), the first dislocation is at the GB and is transformed first into a GBD ($\mathbf{b}_{1/-1}$) emitting an EDisc (shown in the inset). Then, a dipole of EDisc's is created on the right of the GBD; the left EDisc is added to the GBD, forming a dislocation of the lower crystal, while the right EDisc glides away (shown in the inset). In Fig. 5(b), the pileup of dislocations, except the last one, which remains absorbed, has been transmitted, and the remaining EDisc are piling up at the right fixed boundary of the simulated system.

For the mixed dislocation $\mathbf{b}_{1/0}$, the migration of the GB, by creation of EDisc dipoles, occurs before the DPU reaches the GB. As a consequence the DPU follows the GB on its displacement. Therefore, the accommodation of the plastic deformation is produced by the displacement of the GB and the coordinated glide of the DPU.

Since the sense of stress should be reversed if the $\mathbf{b}_{-1/0}$ DPU has to approach the GB, the sense of the displacement of the GB itself is reversed. Therefore, the GB moves against the DPU, inducing the absorption of the first dislocation, creating a $\mathbf{b}_{-2/-1}$ disconnection. Increasing the shear stress allows the absorption of the second dislocation. Eventually, the transmission of two mixed dislocations of the $\langle 100\rangle$ and $1/2\langle 111\rangle$ types is favored.

As initially suggested, an applied shear stress parallel to the GB enhances the creation of EDisc dipoles and therefore facilitates the interactions of the dislocations at the GB.

TABLE II. Local shear stress at the reaction site necessary for triggering a reaction at the interface for the edge dislocations in Cr.

	$\mathbf{b}_{2/0}$	
Temperature (K)	Compression region (MPa)	Tension region (MPa)
300	693	−1543
600	681	−1502
900	646	−1419
	$\mathbf{b}_{-2/0}$	
Temperature (K)	Tension region (MPa)	Compression region (MPa)
300	1399	−549
600	1309	−521
900	825	−426

5. *Interaction in chromium and tungsten*

The reactions presented above depend on crystallographic parameters such as the atomic structure of the interface and the Burgers vector of the dislocations and also on the stress field that controls the distance between dislocations and the threshold stress necessary to create the dipoles of EDisc. Whereas the former condition is related to the bcc structure, the second condition is material dependent.

The interaction of $\mathbf{b}_{2/0}$ and $\mathbf{b}_{-2/0}$ in chromium follow the same pattern as in iron: there is transmission of the dislocations for the $\mathbf{b}_{2/0}$ DPU and shear-coupled GB migration for the $\mathbf{b}_{-2/0}$. Table II presents the local shear stresses parallel to the GB on each side of the interaction region necessary to initiate the reaction; it shows the same tendency as the stresses in Table I.

Tungsten is a good example of how the elastic constants influence the interaction. For this metal, the distance between the first and second dislocations of the DPU is higher than in the other two metals for the same stress applied. This influences the stress field in the interaction region of the GB. For the interaction of the $\mathbf{b}_{2/0}$ DPU, the second dislocation is far from the GBD created by the heading dislocation, and the dipole at the tensile site of the DPU is not created; the GBD acts as a source of single EDiscs, which are responsible for the shear-coupled migration of the GB. No transmission occurs, and the trailing dislocations follow the GB in the displacement. Table III presents the shear stress necessary for the initiation of the *migration* of the GB in tungsten as a function of temperature due to both $\mathbf{b}_{2/0}$ and $\mathbf{b}_{-2/0}$ DPUs.

In order to change the distance between dislocations, looking for a possible transmission, the applied stress in the $\mathbf{b}_{2/0}$ DPU along the glide plane was increased to 3.7 GPa at 300 K. Then, the second dislocation reacted with the GBD originated by the heading dislocation. The reaction is

$$\begin{aligned}\mathbf{b}_{1/-1}+\mathbf{b}_{2/0} &= \tfrac{1}{3}[1\bar{1}2]_\lambda+\tfrac{1}{2}[1\bar{1}1]_\lambda=\cdots\\ &= 3\tfrac{1}{6}[1\bar{1}\bar{1}]_\lambda+[001]_\lambda+\tfrac{1}{3}[1\bar{1}2]_\lambda=\cdots\\ &= 3\mathbf{b}_{1/1}+\mathbf{b}_{2/0}+\mathbf{b}_{-2/-4}. \qquad (3)\end{aligned}$$

TABLE III. Local shear stress at the reaction site necessary for triggering a reaction at the interface for the edge dislocations in W.

	$\mathbf{b}_{2/0}$	
Temperature (K)	Compression region (MPa)	Tension region (MPa)
300	1104	−1733
600	1063	−1575
900	921	−1481
	$\mathbf{b}_{-2/0}$	
Temperature (K)	Tension region (MPa)	Compression region (MPa)
300	2371	−896
600	2104	−820
900	1806	−650

The result is the reflection of a new crystal dislocation (green circle in Fig. 6); no other mechanisms to accommodate the deformation and stress are observed, besides GB migration.

Thus, the final process depends on the balance between the stress necessary to approach two edge dislocations and the stress necessary to create a dipole of EDisc at the GB, i.e., which distribution and level of stresses occurs first.

B. Dislocation pileup–twin interaction

As shown in Sec. IV A, the result of the interaction of a pileup of $1/2\langle 111\rangle$ dislocations with the {112} interface depends on the orientation and sense of the Burgers vector. This dependence affects the interaction of dislocations with the {112} twin. In the following, we consider a twin in Fe formed by two parallel coherent {112} boundaries with variable width. Shear strain increments parallel to the twin are applied, followed by energy minimization of the system.

Figure 7 shows the interaction of a $\mathbf{b}_{2/0}$ DPU with a {112} twin with a thickness of 14 nm, i.e., large enough that the lower TB (TB2) does not affect the interaction at the upper TB (TB1). Since the tensile region of the dislocations is closer to TB1, the DPU is transmitted into the twin. However, the transmitted dislocations inside the twin have an orientation of

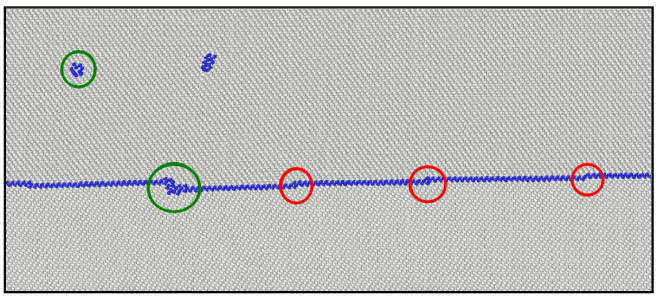

FIG. 6. Snapshot of the interaction of the $\mathbf{b}_{2/0}$ DPU with the {112} GB in W at $T = 300$ K. Defects are indicated with circles, red for EDiscs and green for the $\mathbf{b}_{-2/-4}$ GBD and the $\mathbf{b}_{2/0}$ reflected dislocation.

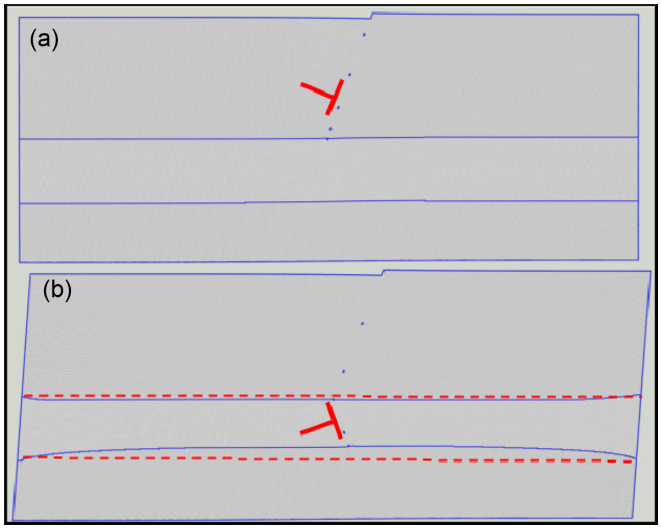

FIG. 7. Snapshots of the interaction of the $\mathbf{b}_{2/0}$ DPU with the $(1\bar{1}2)$ twin with a thickness of 14 nm in Fe. (a) The first dislocation has been absorbed by the upper twin boundary (TB1), producing a $\mathbf{b}_{1/-1}$ TBD. (b) The first and second dislocations of the DPU have been transmitted inside the twin, and the former has already been absorbed by the lower twin boundary (TB2), producing another $\mathbf{b}_{1/-1}$ TBD. Red dashed horizontal lines show the initial thickness of the twin for the sake of comparison.

$\mathbf{b}_{-2/0}$ with respect to TB2; that is, the compression region is closer to the TB, and therefore the dislocation is not transmitted. Instead, the heading dislocation is absorbed by TB2, and it is transformed into a TBD that creates pairs of EDisc that displace the TB upward. The number of dislocations entering into the twin is a function of the width of the twin. The n dislocations inside the twin are stopped by the repulsion of the TBD in TB2. The $(n + 1)$th dislocation of the DPU remains at TB1, emitting a few EDisc that move TB1 down. Altogether, the slip-twin interaction diminishes the width of the twin and accumulates n dislocations inside the twin. Thus, although there is a favorable case for the DPU to be transmitted into the twin, the dislocations cannot come out of it. Therefore, the twin is a barrier for the slip of dislocations.

By diminishing the thickness of the twin to 36–48 (112) planes, the number of transmitted dislocations is reduced to $n = 1$. Then, there are a TBD in TB2, a dislocation absorbed by TB1, and no dislocations inside the twin, as shown in Fig. 8(b). While TB1 emits only a few EDisc, the TBD in TB2 is a profuse source of EDisc that displace TB2 upward up to the total annihilation of the twin.

If the thickness of the twin is less than 36 planes, TB2 influences the interaction of the dislocation with TB1, and there is no transmission of the heading dislocation, which remains in TB1. The stress field created by the dislocation triggers the creation of dipoles of EDiscs in TB2 (as shown in Fig. 3(e) of Ref. [18]) that displace TB2 upward.

Therefore, for twins with a thickness less than 48 planes (5.6 nm), the twin is annihilated, and the dislocation pileup glides freely in the matrix. There is a softening of the material.

If the pileup of dislocations is of the $\mathbf{b}_{-2/0}$ type, for the interaction to occur the sense of stress is reversed. Then

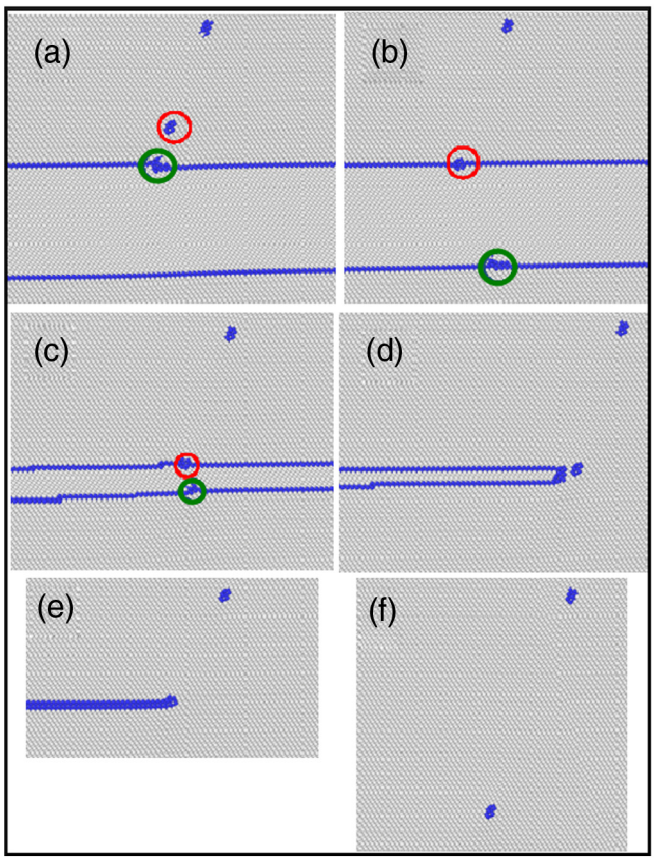

FIG. 8. Snapshots of the interaction of the pileup of $\mathbf{b}_{2/0}$ edge dislocations with the $(1\bar{1}2)$ twin with a thickness of 4.2 nm in Fe. (a) The absorption of the first dislocation of the DPU by the upper twin boundary (TB1) produces a $\mathbf{b}_{1/-1}$ TBD (green circle) with the second dislocation in close proximity (red circle). (b) After the transmission of the first dislocation to the twin it glides up to TB2, where it is absorbed; likewise, the second dislocation is absorbed by TB1. In both interfaces a $\mathbf{b}_{1/-1}$ TBD is produced as a result (red and green circles). (c)–(f) The emission of EDisc dipoles in TB1 and TB2 by the TBDs leads to a progressive reduction of twin thickness up to the total annihilation of the twin.

the leading dislocation approaches TB1, and it is absorbed and transformed into a TBD. In this case, the generation of disconnections displaces TB1 upward against the trailing dislocations, which increases the local stress, which, in turn, triggers the creation of EDisc dipoles in TB2 that displace TB2 downward. Thus, the width of the twin increases. Altogether it represents a strong obstacle for the slip of the pileup, like for the interaction with the {112} GB described above.

The outcome of the DPU-twin interaction is common to the three metals studied. Even in the interaction of $\mathbf{b}_{2/0}$ in W, where the dislocations do not penetrate into the twin, they are stopped by the twin boundary, which results in a strong obstacle.

V. DISCUSSION

Under an applied shear stress, the single $1/2\langle 111\rangle$ dislocation is absorbed by the {112} tilt GB, and it transforms into a GBD that acts as a source of disconnections mediating the shear-coupled migration of the GB. No transmission of the dislocation to the next grain occurs. The scenario changes when a pileup of dislocations interacts with the GB. This is because the trailing dislocations modify the stress field in the interaction region of the heading dislocation with the GB. Then, the transmission of the dislocation occurs if the tensile site of the dislocations (region below the glide plane) is closer to the GB than the compression region ($\mathbf{b}_{2/0}$ dislocation; Fig. 3). Otherwise, the heading dislocation cannot be transmitted, and it behaves as the single $\mathbf{b}_{-2/0}$ dislocation; that is, the absorbed dislocation is transformed into a GBD that mediates the shear-coupled migration. The reason for the different behavior is the location of the disconnection dipoles created at the GB under the stress field of the trailing dislocations, as shown in Figs. 3 and 4. So dislocations with the same orientation of the Burgers vectors but opposite signs perform different interactions. In the $\mathbf{b}_{2/0}$ case, the plastic deformation is accommodated by slip transfer through the GB, and in the $\mathbf{b}_{-2/0}$ case it is accommodated by shear-coupled GB migration. The accommodation of plastic deformation by slip transfer of the $\mathbf{b}_{2/0}$ and $\mathbf{b}_{-1/0}$ dislocations is more efficient since it occurs under lower external shear stress. The shear-coupled migration of the GB, related to $\mathbf{b}_{-2/0}$ and $\mathbf{b}_{1/0}$, is produced against the motion of the dislocation pileup, and therefore, the stresses accumulated at the interaction region are higher.

The above-described behavior is the clue for understanding the slip-twin interaction. The interaction depends on the incident Burgers vector of the pileup, but in any case, there is no transmission across the twin. This is because the dislocations transmitted across the first TB ($\mathbf{b}_{2/0}$), under a shear in the antitwinning direction, have an orientation like $\mathbf{b}_{-2/0}$ with respect to the second TB; therefore, they cannot be transmitted to the matrix. Huang *et al.* [55] reported the same confinement of the dislocations inside the twin in a molecular dynamics simulation of bcc tantalum with coherent twin boundaries under nanoindentation. Reversing the sense of the shear into the twinning direction would approach the $\mathbf{b}_{-2/0}$ dislocation to the twin, and it would not be even transmitted into the twin.

The stress field at the TBs generated by the interacting dislocations enhances the creation of gliding disconnection dipoles at the TBs that displace the TBs either toward each other ($\mathbf{b}_{2/0}$), decreasing the width of the twin (see video 112twin_dislocation_confined.mp4 in the Supplemental Material [56]), or apart from each other ($\mathbf{b}_{-2/0}$), increasing the width of the twin (see video 112twin_growth.mp4 in the Supplemental Material). In the former case, if a maximum of one dislocation from the pileup is transmitted into the twin, the two coherent twin boundaries annihilate and release the dislocation. As a result, the pileup of dislocations has cleaned the thin twins encountered along its glide plane, contributing to the softening of the material (see video 112twin_annihilation.mp4 in the Supplemental Material). In any other case, twins can block the propagation of dislocations and confine dislocations inside the twin, which may contribute to hardening.

Twins represent a strong obstacle for the glide of a pileup of $1/2\langle 111\rangle$ dislocations in two cases: (i) the applied shear is in the twinning direction; (ii) the applied shear is in the

antitwinning direction, and the thickness of the twin is larger than about 48 (112) planes (5.6 nm in Fe).

VI. CONCLUDING REMARKS

The main points of the paper can be summarized as follows:

(i) The interaction of a single dislocation with the {112} tilt grain boundary results in a source of disconnections responsible for the shear-coupled migration of the boundary. No transmission of the dislocation occurs.

(ii) The interaction of a pileup of dislocations with the {112} tilt grain boundary results in either the transmission of the dislocations or shear-coupled grain boundary migration: transmission if the tension region of the dislocation core is close to the boundary, namely, $\mathbf{b}_{2/0}$ and $\mathbf{b}_{-1/0}$, and shear-coupled grain boundary migration if the compression region of the dislocation core is close to the boundary, namely, $\mathbf{b}_{-2/0}$ and $\mathbf{b}_{1/0}$.

(iii) The $1/2\langle 111\rangle$ dislocations are not transmitted across the {112} twins.

(iv) Under shear in the antitwinning direction the slip-twin interaction is as follows: Dislocations of the pileup enter into twins thicker than a few nanometers but remain confined. The number of dislocations accumulating inside the twin is a function of the width of the twin. The interaction contributes to the hardening of the material. Thin twins annihilate due to the displacement of the coherent twin boundaries induced by the interaction with the dislocations, softening the material.

(v) Under shear in the twinning direction, the coherent twin boundary stops the glide of the dislocations that cannot enter the twin, hardening the material.

(vi) The general conclusions related to the atomic processes of the slip-twin interactions are common to the three bcc metals studied, namely, Fe, Cr, and W. Although in the interaction of $\mathbf{b}_{2/0}$ in W the dislocations do not penetrate into the twin, they are stopped by the twin boundary that results in a strong obstacle.

(vii) The differences between metals are related to the interatomic interactions that determine the distribution and magnitude of stresses required in the interaction region to activate the aforementioned processes.

ACKNOWLEDGMENTS

The scientific advice of A. Bakaev in the course of the realization of the present work is gratefully acknowledged. This work was supported by the Euratom Research and Training Programme 2014-2018 under Grant Agreement No. 755039 (Project M4F). This work also contributes to the Joint Program on Nuclear Materials (JPNM) of the European Energy Research Alliance (EERA). This work is partially sponsored by a Belgium FOD fusion grant.

[1] A. Sutton and R. Balluffi, *Interfaces in Crystalline Materials*, 3rd ed., Oxford Classic Texts in the Physical Sciences (Oxford University Press, Oxford, 2006).
[2] J. Wang and A. Misra, Curr. Opin. Solid State Mater. Sci. **15**, 20 (2011).
[3] I. J. Beyerlein, X. Zhang, and A. Misra, Annu. Rev. Mater. Res. **44**, 329 (2014).
[4] G. S. Was, *Fundamentals of Radiation Materials Science*, 2nd ed. (Springer, New York, 2007).
[5] Y. N. Osetsky, D. J. Bacon, F. Gao, A. Serra, and B. N. Singh, J. Nucl. Mater. **283–287**, 784 (2000).
[6] A. Ostapovets and A. Serra, J. Mater. Sci. **52**, 533 (2017).
[7] Z. Cheng, H. Zhou, Q. Lu, H. Gao, and L. Lu, Science **362**, 1925 (2018).
[8] Y. Shen, L. Lu, Q. Lu, Z. Jin, and K. Lu, Scr. Mater. **52**, 989 (2005).
[9] S. Qu, P. Zhang, S. Wu, Q. Zang, and Z. Zhang, Scr. Mater. **59**, 1131 (2008).
[10] S. Kim, X. Li, H. Gao, and S. Kumar, Acta Mater. **60**, 2959 (2012).
[11] J. Wang and X. Zhang, MRS Bull. **41**, 274 (2016).
[12] X. Li, Y. Wei, L. Lu, K. Lu, and H. Gao, Nature (London) **464**, 877 (2010).
[13] T. J. Flanagan, S. Vijayan, S. Galitskiy, J. Davis, B. A. Bedard, C. L. Williams, A. M. Dongare, M. Aindow, and S. W. Lee, Mater. Design **194**, 108884 (2020).
[14] Q. H. Shah, Int. J. Impact Eng. **36**, 1128 (2009).
[15] S. Root, L. Shulenburger, R. W. Lemke, D. H. Dolan, T. R. Mattsson, and M. P. Desjarlais, Phys. Rev. Lett. **115**, 198501 (2015).
[16] A. Serra and D. J. Bacon, Acta Metall. Mater. **43**, 4465 (1995).
[17] A. Serra, N. Kvashin, and N. Anento, Lett. Mater. **10**, 537 (2020).
[18] N. Kvashin, P. L. García-Müller, N. Anento, and A. Serra, Phys. Rev. Mater. **4**, 073604 (2020).
[19] B. P. Eftink, A. Li, I. Szlufarska, N. A. Mara, and I. M. Robertson, Acta Mater. **138**, 212 (2017).
[20] N. Kvashin, N. Anento, D. Terentyev, and A. Serra, Comput. Mater. Sci. **203**, 111044 (2022).
[21] J. P. Hirth and R. C. Pond, Acta Mater. **44**, 4749 (1996).
[22] J. P. Hirth, R. C. Pond, and J. Lothe, Acta Mater. **54**, 4237 (2006).
[23] H. Khater, A. Serra, R. C. Pond, and J. P. Hirth, Acta Mater. **60**, 2007 (2012).
[24] A. Rajabzadeh, M. Legros, N. Combe, F. Mompiou, and D. A. Molodov, Philos. Mag. **93**, 1299 (2013).
[25] A. Rajabzadeh, F. Mompiou, S. Lartigue-Korinek, N. Combe, M. Legros, and D. A. Molodov, Acta Mater. **77**, 223 (2014).
[26] N. Combe, F. Mompiou, and M. Legros, Phys. Rev. B **93**, 024109 (2016).
[27] N. Combe, F. Mompiou, and M. Legros, Phys. Rev. Mater. **1**, 033605 (2017).
[28] N. Combe, F. Mompiou, and M. Legros, Phys. Rev. Mater. **3**, 060601(R) (2019).
[29] Q. Zhu, G. Cao, J. Wang, C. Deng, J. Li, Z. Zhang, and S. X. Mao, Nat. Commun. **10**, 156 (2019).
[30] A. Serra and D. Bacon, Philos. Mag. A **73**, 333 (1996).
[31] N. Kvashin, A. Ostapovets, N. Anento, and A. Serra, Comput. Mater. Sci. **196**, 110509 (2021).

[32] N. Kvashin, N. Anento, D. Terentyev, A. Bakaev, and A. Serra, Phys. Rev. Mater. **5**, 013605 (2021).
[33] L. Wang, Y. Wang, P. Eisenlohr, T. R. Bieler, M. A. Crimp, and D. E. Mason, Metall. Mater. Trans. A **41**, 421 (2010).
[34] D. A. Spearot, K. I. Jacob, and D. L. McDowell, Acta Mater. **53**, 3579 (2005).
[35] C. Y. Hung, Y. Bai, T. Shimokawa, N. Tsuji, and M. Murayama, Sci. Rep. **11**, 8468 (2021).
[36] L. Jiang, M. Arul Kumar, I. J. Beyerlein, X. Wang, D. Zhang, C. Wu, C. Cooper, T. J. Rupert, S. Mahajan, E. J. Lavernia, and J. M. Schoenung, Mater. Sci. Eng., A **759**, 142 (2019).
[37] E. R. Homer, S. M. Foiles, E. A. Holm, and D. L. Olmsted, Acta Mater. **61**, 1048 (2013).
[38] J. S. Weaver, N. Li, N. A. Mara, D. R. Jones, H. Cho, C. A. Bronkhorst, S. J. Fensin, and G. T. Gray, Acta Mater. **156**, 356 (2018).
[39] Y. T. Zhu, X. Z. Liao, and X. L. Wu, Prog. Mater. Sci. **57**, 1 (2012).
[40] Q. H. Tang and T. C. Wang, Acta Mater. **46**, 5313 (1998).
[41] W. Choi, Y. H. Jo, S. S. Sohn, S. Lee, and B. Lee, NPJ Comput. Mater. **4**, 1 (2018).
[42] X. Tian, D. Li, Y. Yu, Z. J. You, T. Li, and L. Ge, Mater. Sci. Eng., A **690**, 277 (2017).
[43] P. Chowdhury and H. Sehitoglu, J. Eng. Mater. Technol. **140**, 020801 (2018).
[44] G. Sainath and B. K. Choudhary, Philos Mag. **96**, 3502 (2016).
[45] M. Mrovec, C. Elsasser, and P. Gumbsch, Philos. Mag. **89**, 3179 (2009).
[46] G. Ackland, M. I. Mendelev, D. J. Srolovitz, S. Han, and A. V. Barashev, J. Phys.: Condens. Matter **16**, S2629 (2004).
[47] D. Terentyev, X. He, A. Serra, and J. Kuriplach, Comput. Mater. Sci. **49**, 419 (2010).
[48] G. Bonny, R. C. Pasianot, D. Terentyev, and L. Malerba, Philos. Mag. **91**, 1724 (2011).
[49] M. C. Marinica, L. Ventelon, M. R. Gilbert, L. Proville, S. L. Dudarev, J. Marian, G. Bencteux, and F. Willaime, J. Phys.: Condens. Matter **25**, 395502 (2013).
[50] A. Stukowski, Modell. Simul. Mater. Sci. Eng. **18**, 015012 (2010).
[51] L. E. Shilkrot, R. E. Miller, and W. A. Curtin, J. Mech. Phys. Solids **52**, 755 (2004).
[52] D. Terentyev, A. Bakaev, A. Serra, F. Pavia, K. L. Baker, and N. Anento, Scr. Mater. **145**, 1 (2018).
[53] P. M. Anderson, J. P. Hirth, and J. Lothe, *Theory of Dislocations*, 3rd ed. (Cambridge University Press, Cambridge, 2017).
[54] N. Anento and A. Serra, Comput. Mater. Sci. **179**, 109679 (2020).
[55] C. Huang, X. Peng, T. Fu, X. Chen, H. Xiang, Q. Li, and N. Hu, Mater. Sci. Eng. A **700**, 609 (2017).
[56] See Supplemental Material at http://link.aps.org/supplemental/10.1103/PhysRevMaterials.6.033606 for the interaction of dislocation pileups with (112) twins.